Neuro-Oncology Advances
5(1), 1–13, 2023 | https://doi.org/10.1093/noajnl/vdad021 | Advance Access date 5 March 2023

MR elastography identifies regions of extracellular matrix reorganization associated with shorter survival in glioblastoma patients

Siri Fløgstad Svensson†, , Skarphéðinn Halldórsson†, Anna Latysheva, Elies Fuster-Garcia, Trine Hjørnevik, Jorunn Fraser-Green, Robin Anthony Birkeland Bugge, Jack Grinband, Sverre Holm, Ralph Sinkus, Einar Osland Vik-Mo and Kyrre Eeg Emblem

Department of Physics and Computational Radiology, Division of Radiology and Nuclear Medicine, Oslo University Hospital, Oslo, Norway (S.F.S., E.F-G., T.H., R.A.B.B., K.E.E.); Department of Physics, University of Oslo, Oslo, Norway (S.F.S., S.Ho.); Vilhelm Magnus Laboratory, Department of Neurosurgery, Oslo University Hospital, Oslo, Norway (S.Ha., E.O.V.-M.); Department of Radiology, Division of Radiology and Nuclear Medicine, Oslo University Hospital, Oslo, Norway (A.L.); BDSLab, Instituto Universitario de Tecnologías de la Información y Comunicaciones, Universitat Politècnica de València, València, Spain (E.F-G.); The Intervention Center, Division for Technology and Innovation, Oslo University Hospital, Oslo, Norway; Department of Radiology, Columbia University, New York, USA (J.G.); Department of Psychiatry, Columbia University, New York, USA (J.G.); Division of Imaging Sciences and Biomedical Engineering, King's College, London, United Kingdom (R.S.); INSERM U1148, LVTS, University Paris Diderot, Paris, France (R.S.)

†Shared first-authorship.

Corresponding Authors: Siri Fløgstad Svensson, MSc., Kyrre Eeg Emblem, PhD., Department for Physics and Computational Radiology, Oslo University Hospital, Building 20, Gaustad sykehus, Sognsvannveien 21, 0372 Oslo, Norway (sirifl@ous-hf.no, kemblem@ous-hf.no).

Abstract

Background. Biomechanical tissue properties of glioblastoma tumors are heterogeneous, but the molecular mechanisms involved and the biological implications are poorly understood. Here, we combine magnetic resonance elastography (MRE) measurement of tissue stiffness with RNA sequencing of tissue biopsies to explore the molecular characteristics of the stiffness signal.

Methods. MRE was performed preoperatively in 13 patients with glioblastoma. Navigated biopsies were harvested during surgery and classified as "stiff" or "soft" according to MRE stiffness measurements ($|G^*|_{norm}$). Twenty-two biopsies from eight patients were analyzed by RNA sequencing.

Results. The mean whole-tumor stiffness was lower than normal-appearing white matter. The surgeon's stiffness evaluation did not correlate with the MRE measurements, which suggests that these measures assess different physiological properties. Pathway analysis of the differentially expressed genes between "stiff" and "soft" biopsies showed that genes involved in extracellular matrix reorganization and cellular adhesion were overexpressed in "stiff" biopsies. Supervised dimensionality reduction identified a gene expression signal separating "stiff" and "soft" biopsies. Using the NIH Genomic Data Portal, 265 glioblastoma patients were divided into those with (n = 63) and without (n = 202) this gene expression signal. The median survival time of patients with tumors expressing the gene signal associated with "stiff" biopsies was 100 days shorter than that of patients not expressing it (360 versus 460 days, hazard ratio: 1.45, $P < .05$).

Conclusion. MRE imaging of glioblastoma can provide noninvasive information on intratumoral heterogeneity. Regions of increased stiffness were associated with extracellular matrix reorganization. An expression signal associated with "stiff" biopsies correlated with shorter survival of glioblastoma patients.

Key Points

- MR elastography can provide unique information on intratumoral heterogeneity preoperatively.
- MR elastography identifies tumor regions of active extracellular reorganization.
- Gene expression signal associated with higher stiffness negatively correlates with survival.

Importance of the Study

Glioblastoma imposes biomechanical forces on the local brain microenvironment, which can affect tumor progression and influence surgical planning; but the identity of the molecular and cellular mechanisms responsible for these forces is not known. Several methods exist to assess tissue stiffness, but MRE is unique in allowing measurements of stiffness *in vivo* and *in situ*. For the first time, we present molecular profiling of glioblastoma tissue correlated with *in vivo* stiffness measurements. The transcriptomic profiles of "stiff" and "soft" biopsies showed that extracellular matrix reorganization was strongly associated with the "stiff" biopsies, in particular collagen binding. Genes associated with innate immune processes were also upregulated in "stiff" biopsies, indicating that these are immunologically active regions of the tumor. The association between gene expression in "stiff" biopsies and survival is in concordance with previous reports of elevated extracellular matrix stiffness increasing glioblastoma aggression.

Intratumoral heterogeneity is characteristic of glioblastoma (GBM) and is believed to be one of the key determinants of therapy failure.[1] It stems from intrinsic genetic alterations as well as the inherent plasticity of GBM tumor cells that adapt to various microenvironmental factors.[2,3] The biomechanical properties of intratumoral heterogeneity are an important factor that can affect how tumor cells interact with the local microenvironment and can contribute to tumor invasion,[4,5] yet, little data exists on the physical characteristics and genetic determinants of biomechanical heterogeneity in GBM. Furthermore, the biomechanical properties of a tumor can be highly variable, with subregions ranging from a soft, gel-like to a dense or solid consistency. Resection of a stiff tumor that adheres to pia and vessels can result in damage to neighboring structures, while soft, liquescent tumors are more readily removed through gentle suction. Thus, differences in biomechanical properties can impact the technical ease of resection and be an important determinant for operative planning.

MR elastography (MRE) is an imaging technique that noninvasively measures the biomechanical properties of tissue. In contrast to intraoperative palpation by the surgeon, MRE provides a quantitative and objective measure of tissue stiffness, and characterizes its spatial distribution. Previous MRE studies in humans have found that GBM tumors differ from healthy brain in terms of shear stiffness and viscosity, and are spatially heterogeneous with respect to measured tissue stiffness.[6,7]

Here, we examine the intratumoral biomechanical heterogeneity of GBM tumors using preoperative MRE and MRI-localized biopsies. Transcriptomic profiling and pathway analysis of "stiff" and "soft" biopsies, as measured by MRE, showed that genes involved in extracellular matrix organization were overexpressed in "stiff" biopsies and were a negative prognostic factor for patient survival. Our data demonstrates that MRE imaging of GBM provides unique information on tumor heterogeneity and helps identify probable regions of active extracellular matrix reorganization.

Methods

This study was approved by the National Research Ethics Committee and the Institutional Review Board (2018/2464 and 2016/1791) and all patients gave written and informed consent. Out of 19 examined patients, four patients were excluded due to technically unsuccessful MRE and one patient was excluded due to MRI susceptibility artifacts caused by an osteosynthesis device. Additionally, one patient was excluded due to failed registration of biopsy coordinates. In total, thirteen patients (eight women and five men, median 56 years, range 38–75 years) with subsequent neuropathologically confirmed IDH wild-type GBM were prospectively included in the study. RNA sequencing was performed on 22 biopsies from eight of these patients.

MR Imaging

MRI exams were performed on a 3T clinical MRI scanner (Ingenia, Philips Medical Systems, Best, the Netherlands) using a 32-channel head coil. In addition to MRE, a clinical preoperative protocol was used, including a T1-weighted

MPRAGE sequence (3D inversion recovery gradient echo, 1 × 1 × 1 mm^3 resolution, 256 × 256 × 368 matrix, TR/TE =5.2/2.3 ms, shot interval 3000 ms, inversion delay 853 ms) acquired before and after administration of a gadolinium-based contrast agent, as well as T2-weighted (turbo spin echo, 0.6 × 0.6 × 4 mm^3 resolution, 420 × 270 × 28 matrix, TR/TE = 3000/80 ms) and T2-FLAIR sequences (turbo spin echo, 1 × 1 × 1 mm^3 resolution, 252 × 249 × 183 matrix, TR/TE = 4800/320 ms, inversion time 1650 ms). For the MRE, a gravitational transducer was attached to the side of the subject's head to induce shear waves of 50 Hz in the brain.[8] Image acquisition was performed using a multi-shot gradient-echo MRE sequence, synchronized to the wave generator by a trigger signal.[9] Fifteen contiguous transversal slices were placed according to the tumor site and scanned using an isotropic resolution of 3.1 mm^3, matrix size of 72 × 70, and FOV = 22 cm. Other scan parameters were: Flip angle = 20°, TR/TE = 384/12 ms, Cartesian readout, and a sensitivity encoding factor of 2. Hadamard motion encoding was performed using bipolar 13 mT/m motion-encoding gradients at 115 Hz in four directions.[10] Eight mechanical phase offsets were acquired throughout the period of the 25-Hz frequency component of the waveform. The actual mechanical vibration frequency was shifted to the second index of the Fourier transform, thus filtering out potential contributions from the 25, 75, and 100 Hz frequencies. The MRE acquisition time was 5.5 min, and was well tolerated across all patients.

Surgery and Tissue Sampling

The surgery was performed by two neurosurgeons. In order to guide sampling, surgeons evaluated MRE data prior to surgery to plan for biopsies covering a range of MRE signal. During resection, 2–7 biopsies were taken from different parts of the tumor. All biopsies were situated in tumor or adjacent parts of the brain that were part of the planned resection prior to MRE evaluation, and included biopsies from contrast-enhancing T1-weighted (CE-T1w), nonenhancing T1-weighted, and T2-FLAIR hyperintense regions. Biopsies were taken early in the resection, as open biopsies, to minimize shift in the navigational accuracy. The biopsy locations were chosen according to varying stiffness as evaluated by the neurosurgeon. The surgeon evaluated tumor consistency according to a modified version of the grading scale from Zada *et al*. as either (1) softer than normal brain tissue, (2) similar in consistency to normal brain tissue, or (3) firmer than normal brain tissue.[11] Stereotactic guidance was provided by preoperative CE-T1w and T2-FLAIR images on a neuronavigation system (Brainlab Curve; Brainlab, Feldkirchen, Germany). The biopsies were snap-frozen immediately after extraction. The frozen biopsies were weighed, homogenized in a Tissuelyser (Qiagen, the Netherlands), and aliquoted for biomolecule extraction.

Biopsy Coregistration

The biopsy locations were recorded by screen captures of the neuronavigation interface at the time of tissue sampling and coregistered to the CE-T1w images using a semiautomated screen capture registration tool, allowing the determination of the Cartesian coordinates of each biopsy.[12] Next, a binary region-of-interest (ROI) mask was created for each biopsy location. Finally, the positions of all ROIs were visually confirmed by an experienced neuroradiologist. The same neuroradiologist also classified each biopsy as (1) contrast-enhancing, (2) necrotic, or (3) nonenhancing with pathological T2-FLAIR signal.

MR Image Processing

From the MRE scan, maps of the magnitude of the shear storage modulus |G*| (tissue stiffness) and the shear phase angle φ (related to tissue viscosity, i.e. its ability to dissipate energy) were produced. Details about the MRE reconstruction can be found in Svensson *et al*.[7] The volumetric CE-T1w images were coregistered to the MRE image space, using a nearest-neighbor interpolation in the nordicICE software (NordicNeuroLab AS, Bergen, Norway). The resulting transformations were applied to the binary ROI masks in CE-T1w space, resulting in a one-voxel seed point in MRE space. To make the analysis more robust to brain shift and coregistration issues, a ROI consisting of a trimmed mean of nine MRE voxels centered on the seed point was used, where the voxel with the highest and the lowest value were removed before averaging. Figure 1A shows an example of a biopsy location on a CE-T1w image and the corresponding |G*| map.

Tissue segmentation was performed using Oncohabitats, a multiparametric system for GBM heterogeneity assessment through MRI.[13] This segmentation was performed for each patient based on pre- and post-contrast T1-weighted, T2-weighted, and T2-FLAIR MRI scans, and resulted in segmentation of contrast-enhancing tumor, necrosis, peritumoral region of T2-FLAIR hyperintensity, and normal-appearing gray and white matter. The mean value of each patient's contralateral normal-appearing white matter was used to normalize MRE measurements, resulting in $|G^*|_{norm}$.[14]

RNA Sequencing

For each patient, 2–4 biopsies were selected for RNA sequencing. Total RNA sequencing returned sequence counts for 22 510 genes and other transcripts. The analyzed biopsies were classified as "stiff" or "soft" based on MRE, i.e., higher or lower $|G^*|_{norm}$ than the average biopsy $|G^*|_{norm}$ within each tumor, respectively. Normalizing measurements to normal-appearing white matter minimized gross differences in stiffness between brains and using relative measurements within each tumor ensured that each patient had at least one biopsy classified as "stiff" and one as "soft." Batch correction of RNA sequencing data was performed with the ComBat-seq package in R.[15] Normalization and differential expression of RNA sequencing data was done with the DESeq2 package in R.[16] The differential expression results were corrected for multiple testing using the Benjamini and Hochberg method, and adjusted *P*-value threshold was set to .05.

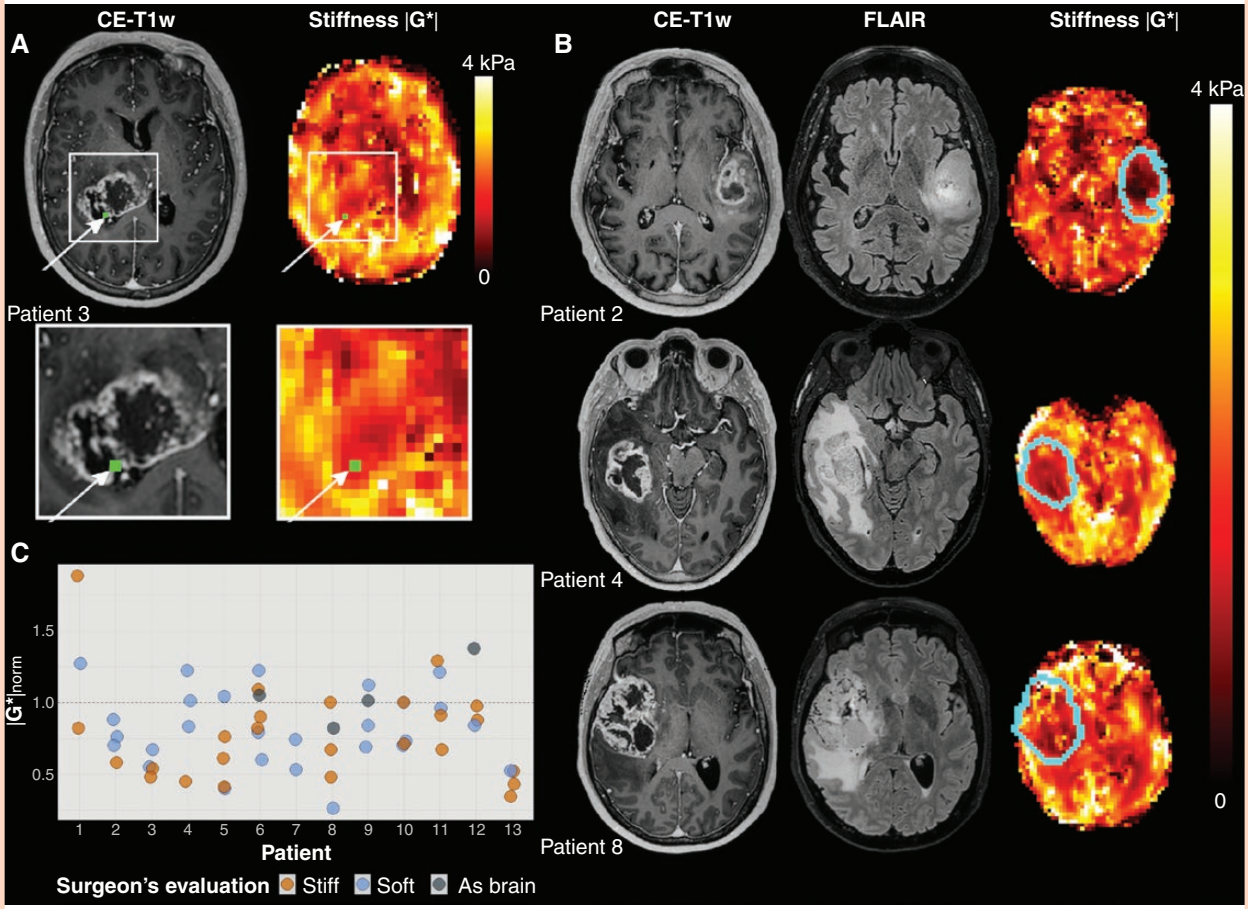

Figure 1. (A)Example of MRE imaging. The location of the tissue biopsy is shown in green in the contrast-enhanced T1-weighted image (CE-T1w) and the MRE stiffness map (|G*|). (B) Representative images for three patients. From left to right: CE-T1w images, and |G*| map, with tumor outline overlaid. (C) Stiffness measurements for all biopsies per patient ($n = 56$). Normalized MRE-based stiffness $|G^*|_{norm}$ for all biopsies acquired for all patients ($n = 13$). The median normalized stiffness for biopsies evaluated by the surgeon as stiff was 0.71, with 0.79 for biopsies evaluated as soft. Biopsies found by the surgeon to be similar in consistency to healthy brain tissue had a median normalized stiffness of 1.03. The horizontal line at $|G^*|_{norm} = 1$ shows the mean stiffness in each patient's contralateral normal-appearing white matter.

Statistical Analysis

Comparison of MRE measurements in tumor and normal-appearing tissue was performed using a Wilcoxon signed-rank test. MRE measurements and tumor volumes were compared using a Spearman's rank order test. $|G^*|_{norm}$ measurements were compared to the surgeon's evaluation using ordered logistic regression and to the radiological tissue type using multinomial regression. A significance level of $P = .05$ was assumed for all tests. Logistic regression was performed using Stata (version 17.0, StataCorp LLC, College Station, Texas, USA). Over-representation (OR) analysis and gene-set enrichment analysis (GSEA) were performed using the clusterProfiler package in R.[17] Principal component analysis (PCA), partial least-squares discriminant analysis (PLS-DA), and sparse PLS-DA were performed with the mixOmics package in R.[18]

Survival analysis

Raw RNA sequencing reads from The Cancer Genome Atlas (TCGA) and the Clinical Proteomic Tumor Analysis Consortium (CPTAC) projects were downloaded from the NIH Genomic Data Commons Data Portal along with sample metadata. Normal samples, control samples, and duplicate samples were excluded, leaving 265 patient samples. Values were batch-corrected with ComBat-seq followed by normalization and rlog transformation in DESeq2. A sparse PLS-DA model containing 22 genes was trained using 22 patient samples, annotated as "stiff" or "soft," using the mixOmics package. Expression of these 22 genes was used to classify the external data using the "predict()" function in the mixOmics package. Kaplan–Meier survival curves were produced with the survminer package in R. Cox regression analysis on survival data was performed in SPSS (version 28.0, IBM Corp, Armonk, NY).

Code and Data Availability

The source code and data to reproduce all analyses and figures in this manuscript are available at https://github.com/SkabbiVML/stiffR.

Table 1. Biopsies Used in RNA Sequencing

Patient Number	Sample Number	Tissue Type	Surgeon's Evaluation	$\|G^*\|_{norm}$	MRE Soft/Stiff
1	1	CE	Stiff	0.82	"Soft"
	2	FLAIR	Stiff	1.88	"Stiff"
	3	CE	Soft	1.27	"Soft"
2	1	FLAIR	Soft	0.76	"Soft"
	2	CE	Soft	0.88	"Stiff"
	3	CE	Soft	0.70	"Soft"
3	1	CE	Soft	0.67	"Stiff"
	2	Necrosis	Stiff	0.54	"Soft"
	3	Necrosis	Stiff	0.48	"Soft"
4	1	FLAIR	Soft	1.22	"Stiff"
	2	CE	Soft	1.01	"Stiff"
	3	Necrosis	Stiff	0.45	"Soft"
5	1	FLAIR	Soft	0.40	"Soft"
	2	Necrosis	Soft	1.04	"Stiff"
	3	CE	Stiff	0.76	"Stiff"
6	1	CE	Soft	0.79	"Stiff"
	2	CE	Soft	0.60	"Soft"
	3	CE	Stiff	0.82	"Stiff"
7	1	CE	Soft	0.53	"Soft"
	2	CE	Soft	0.74	"Stiff"
8	1	CE	Stiff	1.00	"Stiff"
	2	CE	Stiff	0.48	"Soft"

The tissue type of each biopsy point was radiologically evaluated, using CE-T1w and T2-FLAIR images, as contrast-enhancing tumor (CE), region with high signal on T2-FLAIR (FLAIR) or necrosis. Surgeon's evaluation of the consistency of each biopsy (stiff or soft compared to normal brain parenchyma), $|G^*|_{norm}$, and MRE biopsy classification ("stiff" or "soft," i.e. higher or lower $|G^*|_{norm}$ than the mean value of all biopsies within each tumor, respectively).

Results

The demographic data of the patients, tumor volumes, and mean $|G^*|_{norm}$ and φ_{norm} values are listed in Supplementary Table 1. Example MRE images are shown in Figure 1B.

GBM Tumors are Heterogeneous and Softer than Normal-appearing Brain Tissue

The mean stiffness $|G^*|$ was 20% lower in contrast-enhancing tumor than in normal-appearing white matter ($P < .001$) and 30% lower in necrotic tissue than normal-appearing white matter ($P < .001$). The mean shear phase angle φ was 10% lower in contrast-enhancing tumor than in normal-appearing white matter ($P < .001$) and 8% lower in necrotic tissue than in normal-appearing white matter ($P < 0.005$). In the nonenhancing T2-FLAIR hyperintense regions, stiffness did not differ significantly from normal-appearing white matter ($P = .8$), but φ was 15% lower than in normal-appearing white matter ($P < .001$). The median tumor volume (contrast-enhancing and necrotic regions combined) was 33 cm^3 (range 7–78 cm^3), and the median volume of the T2-FLAIR hyperintensity was 45 cm^3 (range 2–162 cm^3). Mean $|G^*|_{norm}$ and φ_{norm} values did not correlate with the volume of tumor or edema.

The stiffness was heterogeneous both within and between tumors (Figure 1C). Some patients (e.g., patient 13) had $|G^*|_{norm}<1$ for all biopsies, while others displayed higher stiffness values for some biopsies (e.g., patient 1). The median ratio between the biopsy with highest and lowest stiffness of a patient was 1.6 (range 1.4-3.9). Table 1 shows $|G^*|_{norm}$ and the surgeon's evaluation of biopsies that were analyzed by RNA sequencing. The table also shows whether the biopsy was taken from contrast-enhancing tumor, necrosis, or T2-FLAIR hyperintensity. Measured stiffness $|G^*|_{norm}$ did not differ significantly between radiological tissue classes ($P = .06$).

The surgeon's evaluation of biopsy stiffness during surgery and $|G^*|_{norm}$ did not correlate ($P = .58$), suggesting that the measures represent different physiological properties.

Gene Expression associated with GBM Stiffness

To evaluate the molecular differences between "stiff" and "soft" tissue biopsies, we performed total RNA

sequencing on 22 biopsies from 8 GBM tumors (patients 1–8). The measurements of the biopsy $|G^*|_{norm}$ compared to the distribution of $|G^*|_{norm}$ in all voxels are shown in Supplementary Fig. 1.

Unsupervised dimensionality reduction by principal component analysis (Supplementary Fig. 2A) did not identify tissue stiffness as measured by MRE as a strong source of variance within the data. However, supervised dimensionality-reduction with partial least-squares discriminant analysis (PLS-DA) identified an expression signal that separated "stiff" from "soft" biopsies within each tumor. Tuning of the PLS-DA parameters (5-fold cross-validation, 100 repeats) indicated that a minimal sparse PLS-DA model containing 22 genes was sufficient to separate 22 patient samples based on the measured tissue stiffness (Supplementary Fig. 2C).

Differential gene expression analysis between "stiff" and "soft" biopsies per patient found that 196 genes were differentially expressed based on an adjusted *P*-value of .05 (Figure 3A, Supplementary Table 3). Of these, 122 genes were upregulated in "stiff" biopsies, while 74 were upregulated in "soft" biopsies. Normalized expression levels of differentially expressed genes in every biopsy show that "stiff" or "soft" biopsies tend to cluster together, and biopsies within individual patients show similar expression profiles (Figure 2B). Due to the limited size of the dataset, differential expression may depend on samples from a single patient. Therefore, to explore the robustness of the differential expression, we performed sequential differential expression analysis, leaving out all samples from a single patient in each iteration. Patient-wise leave-one-out cross-validation identified a set of 43 genes (35 in "stiff" biopsies and 8 in "soft" biopsies) that were found to be differentially expressed on every iteration (Table 2). Repeating this analysis after classifying biopsies into "stiff" or "soft" using the surgeon's intraoperative evaluation did not show significant differences in gene expression.

Functional Annotation of Stiffness-associated Gene Expression

To evaluate the structural and functional importance of differentially expressed genes, we performed a gene set enrichment analysis (GSEA) of genes associated with higher biopsy stiffness using the Gene Ontology (GO) and Reactome databases.[19,20] The GO-terms with the highest association to "stiff" biopsies represent components of the extracellular matrix, cellular adhesion, and innate immunity (Figure 3A). Similarly, among the most significantly enriched Reactome pathways associated with "stiff" biopsies were extracellular matrix organization, integrin cell-surface interactions, and neutrophil degranulation (Supplementary Fig. 3). In contrast, GO-terms and Reactome pathways with highest association with "soft" biopsies largely represented normal neuronal functions, such as regulation of membrane potential and neurotransmitter receptor complex, although associations to DNA methylation and rRNA regulation were also found. Pathway enrichment maps show three distinct clusters of GO-terms with varying degrees of overlap. GO-terms associated with extracellular matrix reconstruction were upregulated in "stiff" samples. There is some overlap of genes associated with extracellular matrix terms and terms associated with effector cells of the innate immune system (neutrophils and granulocytes) which were also upregulated in stiff samples (Figure 3B). A third cluster of pathways, representing neuronal synapses and synaptic membranes, was upregulated in "soft" biopsies.

Over-representation analysis of the 196 genes found to be upregulated in "stiff" or "soft" biopsies (adjusted *P*-value < .05, Supplementary Table 3) was largely concordant with the results from the GSEA: "Stiff" biopsies were associated with collagen-containing matrix reorganization, focal adhesion, and immune cell activation/migration, while "soft" biopsies were associated with normal synaptic activity and, to a lesser extent, DNA packaging and nucleosomes. Over-representation analysis of Reactome pathways identified "extracellular matrix organization" as strongly associated with "stiff" biopsies while DNA methylation and RNA polymerase I promoter opening were associated with "soft" biopsies (Supplementary Fig. 4).

Tissue Stiffness is a Negative Prognostic Factor for Patient Survival

Extracellular matrix reorganization and increased tissue stiffness have been associated with tumor cell infiltration in glioma.[5] Based on our findings, we hypothesized that regions of higher stiffness are important for GBM progression and hence patient survival. To further study the effect of the gene expression signal that distinguished our "stiff" and "soft" biopsies, we evaluated RNA transcription profiles of 265 GBM tumors from two studies available in the NIH Genomic Data Commons Data Portal (168 biopsies from TCGA and 97 biopsies from CPTAC).[21] Expression patterns of the 22 stable genes selected by PLS-DA were used to classify the tumors *with* this gene expression signal (n = 63) and tumors *without* it (n = 202). Survival analysis showed that the median survival time of patients carrying tumors expressing this gene signal was 100 days shorter than that of patients without this gene expression signal, from a median of 460 to 360 days (Figure 4). Cox regression analysis showed that this gene expression signal had a significant impact on survival, with a 45% higher risk of death at any given time for patients with this gene expression signal (Supplementary Table 2). This result was significant after adjusting for age, sex, and type of treatment (hazard ratio: 1.45, 95% confidence interval: 1.043–2.015, $P < 0.05$).

Discussion

Our study compared the transcriptomic profiles of "stiff" and "soft" GBM tissue biopsies as measured by MRE. We found that extracellular matrix reorganization, focal adhesion, and neutrophile-mediated immune responses were associated with higher stiffness within the tumor. Our quantitative measure of stiffness in each biopsy location did not correlate with the surgeon's subjective evaluation based on palpation. The "stiff" and "soft" biopsies, as quantified by MRE, could be separated by a gene

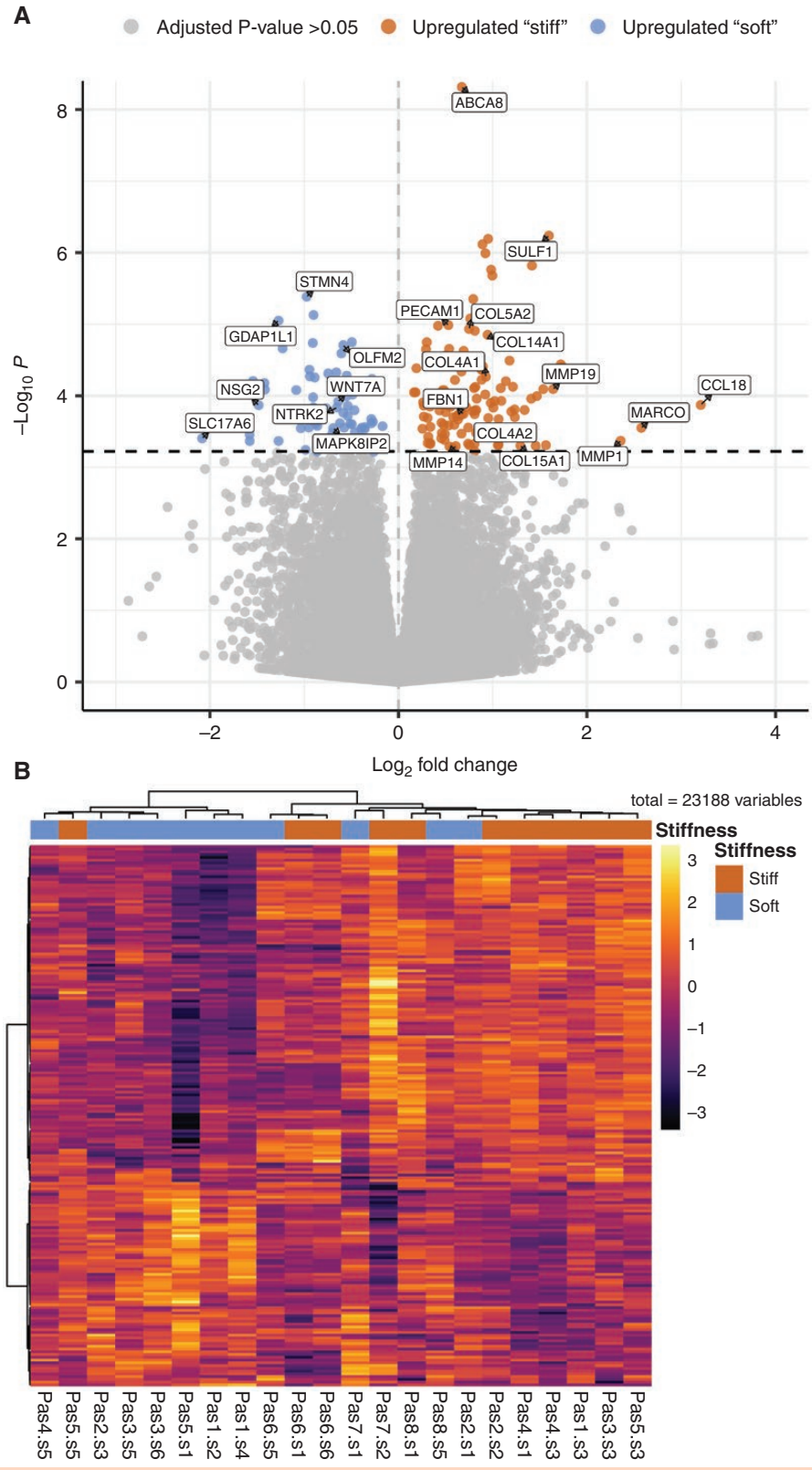

Figure 2. Differential gene expression between "stiff" and "soft" biopsies in GBM tumors. (A) Volcano plot summarizing the results of differential gene expression between "stiff" and "soft" biopsies. The magnitude of change in expression between "stiff" and "soft" biopsies is shown along the x-axis, and the statistical significance is shown along the y-axis. About 521 genes were found to have differential expression between the groups with an adjusted *P*-value < .1, 196 genes with an adjusted *P*-value < .05 shown in blue and red. (B) Heatmap of differentially expressed genes, where biopsies are grouped according to the pattern of gene expression. All genes that passed an adjusted *P*-value threshold of .05 (196 genes) are included in the heat map, along the y-axis. The analyzed biopsies are shown along the x-axis. The color gradient shows the changes of gene expression, the expression of genes is scaled across all biopsies. "Pas" represents patient number, "s" represents biopsy number.

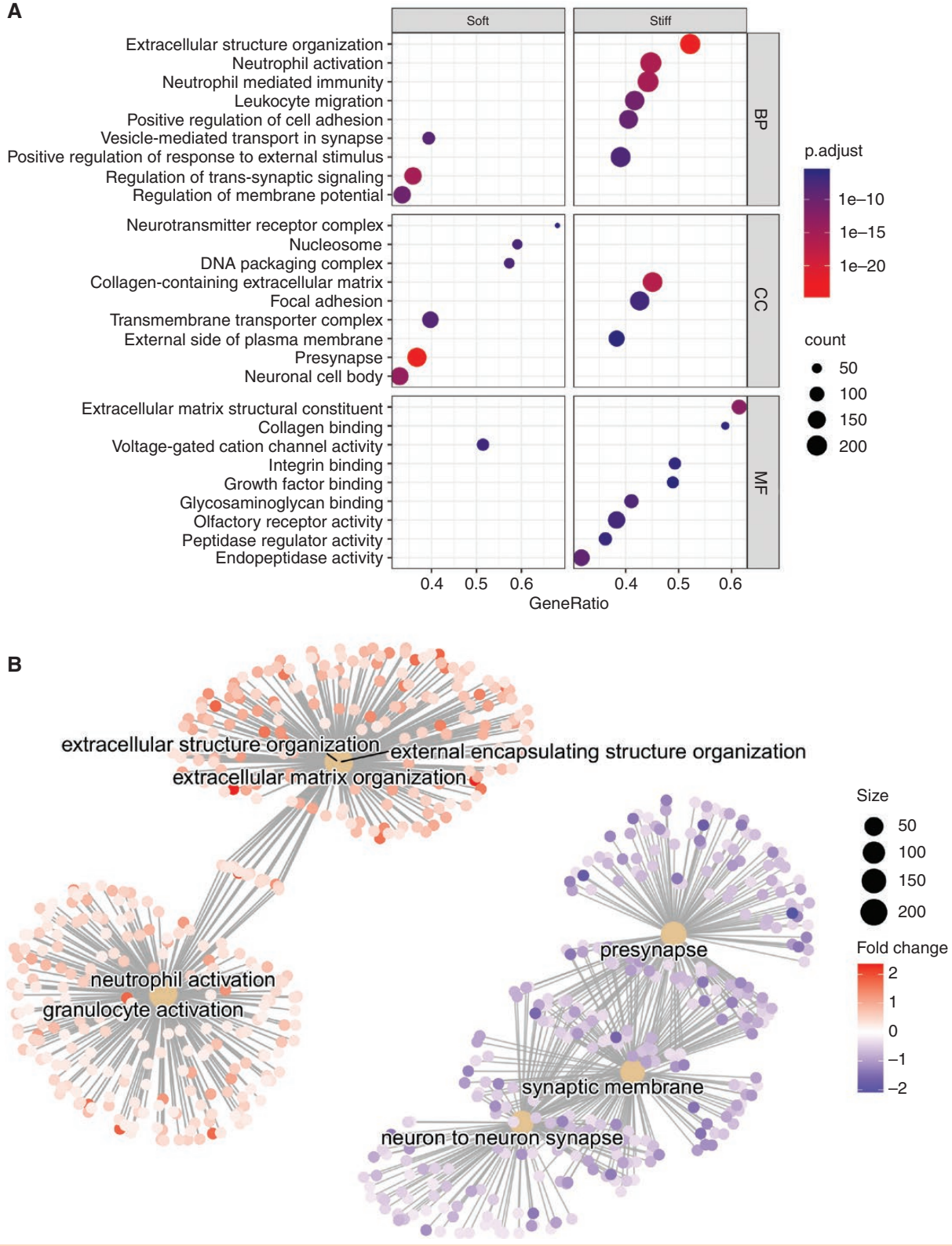

Figure 3. Gene-set enrichment analysis of differentially expressed genes in "soft" and "stiff" tumor biopsies. (A) Dot plot representing the terms most highly enriched in each Gene Ontology category. BP = Biological process, CC = cellular component, MF = molecular function, p.adjust = *p*-value adjusted for multiple testing. (B) Pathway enrichment map of the GSEA results. Central nodes represent Gene Ontology terms, smaller dots represent differentially expressed genes (>0= upregulated in "stiff" biopsies, <0 = upregulated in "soft" biopsies").

Table 2. Differentially Expressed Genes: List of Most Stable Differentially Expressed Genes between "Stiff" and "Soft" Biopsies after Patient-wise Leave-one-out Validation

ENTREZ ID	Gene ID	Association	Gene Name
84935	MEDAG	"Stiff"	Mesenteric estrogen dependent Adipogenesis
1378	CR1	"Stiff"	Complement C3b/C4b receptor 1 (Knops blood group)
23213	SULF1	"Stiff"	Sulfatase 1
3875	KRT18	"Stiff"	Keratin 18
9332	CD163	"Stiff"	CD163 molecule
100628315	DNM3OS	"Stiff"	DNM3 opposite strand/antisense RNA
728264	CARMN	"Stiff"	Cardiac mesoderm enhancer-associated noncoding RNA
5325	PLAGL1	"Stiff"	PLAG1 like zinc finger 1
8829	NRP1	"Stiff"	Neuropilin 1
54885	TBC1D8B	"Stiff"	TBC1 domain family member 8B
7373	COL14A1	"Stiff"	Collagen type XIV alpha 1 chain
1282	COL4A1	"Stiff"	Collagen type IV alpha 1 chain
79839	CCDC102B	"Stiff"	Coiled-coil domain containing 102B
1601	DAB2	"Stiff"	DAB adaptor protein 2
3672	ITGA1	"Stiff"	Integrin subunit alpha 1
4121	MAN1A1	"Stiff"	Mannosidase alpha class 1A member 1
55075	UACA	"Stiff"	Uveal autoantigen with coiled-coil domains and ankyrin repeats
5205	ATP8B1	"Stiff"	ATPase phospholipid transporting 8B1
5139	PDE3A	"Stiff"	Phosphodiesterase 3A
22925	PLA2R1	"Stiff"	Phospholipase A2 receptor 1
5592	PRKG1	"Stiff"	Protein kinase cGMP-dependent 1
1909	EDNRA	"Stiff"	Endothelin receptor type A
1290	COL5A2	"Stiff"	Collagen type V alpha 2 chain
1368	CPM	"Stiff"	Carboxypeptidase M
9060	PAPSS2	"Stiff"	3′-phosphoadenosine 5′-phosphosulfate synthase 2
10351	ABCA8	"Stiff"	ATP binding cassette subfamily A member 8
8654	PDE5A	"Stiff"	Phosphodiesterase 5A
3759	KCNJ2	"Stiff"	Potassium inwardly rectifying channel subfamily J member 2
5175	PECAM1	"Stiff"	Platelet and endothelial cell adhesion molEcule 1
2321	FLT1	"Stiff"	Fms related receptor tyrosine kinase 1
115548	FCHO2	"Stiff"	FCH and mu domain containing endocytic adaptor 2
84910	TMEM87B	"Stiff"	Transmembrane protein 87B
9169	SCAF11	"Stiff"	SR-related CTD associated factor 11
23216	TBC1D1	"Stiff"	TBC1 domain family member 1
2803	GOLGA4	"Stiff"	Golgin A4
875	CBS	"Soft"	Cystathionine beta-synthase
728875	LINC00623	"Soft"	Long intergenic non-protein coding RNA 623
93145	OLFM2	"Soft"	Olfactomedin 2
1600	DAB1	"Soft"	DAB adaptor protein 1
767	CA8	"Soft"	Carbonic anhydrase 8
441381	LRRC24	"Soft"	Leucine rich repeat containing 24
81551	STMN4	"Soft"	Stathmin 4
345630	FBLL1	"Soft"	Fibrillarin like 1

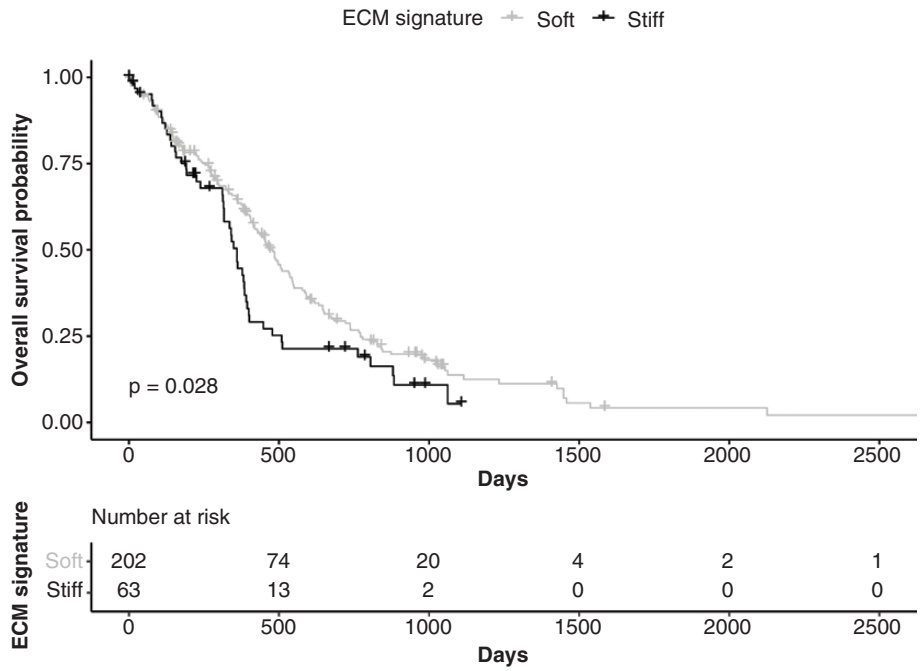

Figure 4. Survival analysis using data from TCGA and CPTAC. The median survival time of patients carrying tumors expressing the 22 genes associated with "stiff" biopsies ($n = 63$, shown in black) was 100 days shorter than that of patients who did not express these genes ($n = 202$, shown in gray).

expression signal of 22 genes. Finally, we showed that the expression signal found in "stiff" biopsies is associated with shorter survival times in patients with GBM.

Previous MRE studies on GBM tumors have reported lower mean tumor stiffness of GBM compared to radiographically normal-appearing white matter.[6] This is in accordance with our findings that tumor tissue is on average softer than contralateral white matter. However, the stiffness within each tumor was also highly variable, containing regions of high and low value compared to normal-appearing tissue.

The heterogeneity in tissue stiffness in and around GBM *in vivo* is not well understood. At the single-cell level, glioma cells have been measured to be stiffer than normal brain cells.[22,23] Similarly, several studies using atomic force microscopy (AFM) report that GBM tissue is stiffer than nontumor tissue.[24–26] However, GBM has also been reported to be softer than the normal brain using AFM in animal models,[27] and GBM cells have been reported to be softer than normal fibroblasts.[28]

Hence, the measured stiffness in GBM varies both with the method and scale at which it is measured. In contrast to MRE, AFM is an indentation method, which probes the tissue in a quasi-static manner.[26] As the viscoelastic properties of tissue depend on the frequency at which they are measured, different results in AFM and MRE studies should be expected.[29] In addition, tissue in pathological states may have different frequency characteristics. Thus, the contrast between healthy and pathological tissue may differ between AFM and other microrheology techniques operating at zero frequency, and MRE. In contrast to these *in vitro* methods, MRE uniquely measures tissue stiffness *in vivo* and *in situ*.

A major source of tissue stiffening in GBM has been hypothesized to be restructuring of the extracellular matrix, though definitive evidence had not been available.[24] To the best of our knowledge, this study is the first to characterize the transcriptomic profiles of "stiff" and "soft" biopsies and demonstrate that tissue stiffness is associated with extracellular matrix reorganization, particularly, collagen-related processes. Levels of fibrillar collagens in the healthy brain are low compared to the rest of the body, but in glioma, collagen levels are elevated and play a vital role in driving tumor progression.[30] Gene sets associated with innate immune processes, such as neutrophil activation, were also upregulated in "stiff" biopsies, indicating that these are active regions of the tumor.[31] Thus, our findings support the idea that as the tumor progresses, it remodels its environment, producing a stiffening of the extracellular matrix. Elevated extracellular matrix stiffness has been shown to increase GBM aggression[24] and proliferation.[5,32] Several of the genes we found to be upregulated in "stiff" biopsies have previously been shown to play a role in glioma malignancy. *NRP1* and *DAB2* have been linked to glioma progression,[33,34] *PECAM1* correlates with GBM aggressiveness,[35] *CD163* is positively associated with the glioma malignancy grade,[36] and *Flt1* promotes invasion and migration of GBM cells.[37] *CR1, PLAGL1, COL4A1*, and *COL5A2* have all been shown to correlate with shorter survival.[38–41]

When our data was compared to previously published transcriptomic profiles of GBM samples, we found that

median survival was significantly shorter in patients with tumors exhibiting the gene expression signal associated with "stiff" biopsies. This indicates that the genetic and molecular processes we detect in "stiff" tumor biopsies play a role in the malignant progression of GBM tumors. These results are concordant with Miroshnikova *et al.* who reported a significant correlation between the proportion of highly stiff ECM areas within a GBM tumor and worse patient prognosis, suggesting that elevated ECM stiffness can foster GBM aggression.[24]

In contrast to AFM, MRE provides a stiffness map of the entire tumor and the surrounding tissue, and is therefore uniquely able to capture the heterogeneity of the biomechanical properties of a tumor prior to surgery. Previous work comparing the evaluation of tumor stiffness by neurosurgeons with MRE in meningiomas and in pituitary adenomas found that the measured stiffness correlated positively with the surgeon's evaluation.[42,43] However, in these studies, the mean stiffness value for the entire tumor was reported. From tumor to tumor, meningiomas are known to vary in stiffness, from very firm to very soft.[42] In patients with gliomas, surgeons' haptic impressions have been found to vary widely and therefore have not been suitable as a gold standard of tumor consistency.[44] This illustrates the challenge of comparing MRE measurements with surgeons' impression, especially for small ROIs. MRE probes the shear properties of tissue, whereas probing by surgical tools is a different process. In addition to the surgeon's probing operating at zero frequency, the tissue can be compressed and compromised. Furthermore, tumor growth can compress surrounding tissue, generating solid stress due to swelling.[45,46] Several studies have found that MRE is sensitive to compressive stress.[47,48] Opening the skull during a craniotomy changes the pressure conditions in the brain, which may affect the perceived tissue stiffness compared to MRE measurements performed while the skull is still intact. When classifying biopsies using the surgeons' evaluation rather than MRE, no significant difference in gene expression was found between biopsies evaluated as "stiff" and "soft."

Our study is not without limitations. First, since the number of patients included in the analysis is relatively low, it has not been possible to explore factors that are known to affect overall survival, such as IDH mutation status, treatment effects, sex, etc. Therefore, our findings should be validated in a larger patient cohort. Second, perfect accuracy between preoperative imaging and biopsy locations is difficult to achieve, as brain shift can occur when the cranium is opened. All biopsies were collected prior to bulk resection, thereby minimizing registration errors between preoperative imaging and biopsy location. The effect of such errors was further reduced by dilating the biopsy voxel and averaging the MRE signal across voxels within the ROI. Third, because the external data sets used to perform the survival analysis did not contain any MRE data, it is not possible to know whether those tumors were stiff or soft; rather, we can only conclude that the gene expression signal associated with stiffness and extracellular matrix reorganization, is also associated with worse overall survival.

In conclusion, MRE identifies regions of malignant extracellular matrix reorganization with an expression signal correlated to shorter survival time in patients with GBM. Thus, MRE may be a powerful tool for characterizing tumor heterogeneity during presurgical planning.

Supplementary Material

Supplementary material is available online at *Neuro-Oncology Advances* online.

Keywords

biomechanics | elastography | extracellular matrix | glioblastoma | stiffness

Funding

We gratefully acknowledge support from the European Union's Horizon 2020 Programme: ERC Grant [758657-ImPRESS], Research and Innovation Grant [668039-FORCE], Marie Skłodowska-Curie grant [844646-GLIOHAB]; South-Eastern Norway Regional Health Authority [2017073, 2013069, 2021057]; The Research Council of Norway Grant [261984, 325971]; the National Institutes of Health R21 grant [EB030757]; the German Research Foundation [SCHR 1542/1-1]; the Spanish State Research Agency, Subprogram for Knowledge Generation [PROGRESS, No PID2021-127110OA-I00].

Conflict of interest statement. **K.E.E.:** NordicNeuroLab AS, Bergen, Norway – Intellectual property rights. R.A.B.B.: GE Healthcare, Chicago, Illinios, USA – Consultant work. S.F.S.: No conflict of interest, S.Ha.: No conflict of interest, A.L.: No conflict of interest, E.F-G.: No conflict of interest, T.H.: No conflict of interest, JFG: No conflict of interest, JG: No conflict of interest, S.Ho.: No conflict of interest, R.S.: No conflict of interest, E.O.V-M.: No conflict of interest.

Authorship statement. Study design: S.F.S., S.Ha., E.O.V-M., K.E.E. Data collection: S.F.S., S.Ha., J.F-G, R.A.B.B., E.O.V-M.. Data analysis: S.F.S., S.Ha., A.L., E.F-G., T.H., J.G. Data interpretation: S.F.S., S.Ha., AL, S.Ho., R.S., E.O.V-M., K.E.E. Writing/approving final manuscript: all authors.

References

1. Qazi MA, Vora P, Venugopal C, et al. Intratumoral heterogeneity: pathways to treatment resistance and relapse in human glioblastoma. *Ann Oncol.* 2017; 28(7):1448–1456.
2. Lombardi MY, Assem M. Glioblastoma genomics: a very complicated story. In: De Vleeschouwer S, ed. *Glioblastoma.* Brisbane, Australia: Codon Publications; 2017.

3. Dirkse A, Golebiewska A, Buder T, et al. Stem cell-associated heterogeneity in Glioblastoma results from intrinsic tumor plasticity shaped by the microenvironment. *Nat Commun*. 2019; 10(1):1787.
4. Ciasca G, Sassun TE, Minelli E, et al. Nano-mechanical signature of brain tumours. *Nanoscale*. 2016; 8(47):19629–19643.
5. Ulrich TA, de Juan Pardo EM, Kumar S. The mechanical rigidity of the extracellular matrix regulates the structure, motility, and proliferation of glioma cells. *Cancer Res*. 2009; 69(10):4167–4174.
6. Bunevicius A, Schregel K, Sinkus R, Golby A, Patz S. REVIEW: MR elastography of brain tumors. *Neuroimage Clin*. 2019; 25:102109. https://doi.org/10.1016/j.nicl.2019.102109.
7. Svensson SF, Fuster-Garcia E, Latysheva A, et al. Decreased tissue stiffness in glioblastoma by MR elastography is associated with increased cerebral blood flow. *Eur J Radiol*. 2022; 147:110136. doi: 10.1016/j.ejrad.2021.110136.
8. Runge JH, Hoelzl SH, Sudakova J, et al. A novel magnetic resonance elastography transducer concept based on a rotational eccentric mass: preliminary experiences with the gravitational transducer. *Phys Med Biol*. 2019; 64(4):045007.
9. Guenthner C, Sethi S, Troelstra M, et al. Ristretto MRE: a generalized multi-shot GRE-MRE sequence. *NMR Biomed*. 2019; 32(5):e4049.
10. Guenthner C, Runge JH, Sinkus R, Kozerke S. Analysis and improvement of motion encoding in magnetic resonance elastography. *NMR Biomed*. 2018; 31(5):e3908.
11. Zada G, Yashar P, Robison A, et al. A proposed grading system for standardizing tumor consistency of intracranial meningiomas. *Neurosurg Focus*. 2013; 35(6):E1.
12. Petridis PD, Horenstein CI, Pereira B, et al. BOLD asynchrony elucidates tumor burden in IDH-mutated gliomas. *Neuro Oncol*. 2022; 24(1):78–87.
13. Juan-Albarracin J, Fuster-Garcia E, Manjon JV, et al. Automated glioblastoma segmentation based on a multiparametric structured unsupervised classification. *PLoS One* .2015; 10(5):e0125143.
14. Svensson SF, De Arcos J, Darwish OI, et al. Robustness of MR elastography in the healthy brain: repeatability, reliability, and effect of different reconstruction methods. *J Magn Reson Imaging*. 2021; 53(5):1510–1521.
15. Zhang Y, Parmigiani G, Johnson WE. ComBat-seq: batch effect adjustment for RNA-seq count data. *NAR Genom Bioinformat*. 2020; 2(3):lqaa078.
16. Love MI, Huber W, Anders S. Moderated estimation of fold change and dispersion for RNA-seq data with DESeq2. *Genome Biol*. 2014; 15(12):550.
17. Yu G, Wang L-G, Han Y, He Q-Y. clusterProfiler: an R package for comparing biological themes among gene clusters. *OMICS*. 2012; 16(5):284–287.
18. Rohart F, Gautier B, Singh A, Lê Cao K-A. mixOmics: an R package for 'omics feature selection and multiple data integration. *PLoS Comput Biol*. 2017;13(11):e1005752–e1005752.
19. Gene Ontology C. The Gene Ontology resource: enriching a GOld mine. *Nucleic Acids Res*. 2021; 49(D1):D325–D334.
20. Gillespie M, Jassal B, Stephan R, et al. The reactome pathway knowledgebase 2022. *Nucleic Acids Res*. 2022; 50(D1):D687–D692.
21. Grossman RL, Heath AP, Ferretti V, et al. Toward a shared vision for cancer genomic data. *N Engl J Med*. 2016; 375(12):1109–1112.
22. KhanZS, VanapalliSA. Probing the mechanical properties of brain cancer cells using a microfluidic cell squeezer device. *Biomicrofluidics*.2013;7(1):11806.
23. Graybill PM, Bollineni RK, Sheng Z, Davalos RV, Mirzaeifar R. A constriction channel analysis of astrocytoma stiffness and disease progression. *Biomicrofluidics*. 2021; 15(2):024103.
24. Miroshnikova YA, Mouw JK, Barnes JM, et al. Tissue mechanics promote IDH1-dependent HIF1α–tenascin C feedback to regulate glioblastoma aggression. *Nat Cell Biol*. 2016; 18(12):1336–1345.
25. Chen X, Wanggou S, Bodalia A, et al. A feedforward mechanism mediated by mechanosensitive ion channel PIEZO1 and tissue mechanics promotes glioma aggression. *Neuron*. 2018; 100(4):799–815.e7.
26. Ciesluk M, Pogoda K, Deptula P, et al. Nanomechanics and histopathology as diagnostic tools to characterize freshly removed human brain tumors. *Int J Nanomedicine*. 2020; 15:7509–7521. doi: 10.2147/IJN.S270147. eCollection 2020.
27. Seano G, Nia HT, Emblem KE, et al. Solid stress in brain tumours causes neuronal loss and neurological dysfunction and can be reversed by lithium. *Nat Biomed Eng*. 2019; 3(3):230–245.
28. Ning D, Duong B, Thomas G, et al. Mechanical and morphological analysis of cancer cells on nanostructured substrates. *Langmuir*. 2016; 32(11):2718–2723.
29. Parker KJ, Szabo T, Holm S. Towards a consensus on rheological models for elastography in soft tissues. *Phys Med Biol*. 2019; 64(21):215012–215012.
30. Payne LS, Huang PH. The pathobiology of collagens in glioma. *Mol Cancer Res*. 2013; 11(10):1129–1140.
31. Lin Y-J, Wei K-C, Chen P-Y, Lim M, Hwang T-L. Roles of neutrophils in glioma and brain metastases. *Front Immunol*. 2021; 12: Article 701383 https://doi.org/10.3389/fimmu.2021.701383.
32. Umesh V, Rape AD, Ulrich TA, Kumar S. Microenvironmental stiffness enhances glioma cell proliferation by stimulating epidermal growth factor receptor signaling. *PLoS One*. 2014; 9(7):e101771.
33. Hu B, Guo P, Bar-Joseph I, et al. Neuropilin-1 promotes human glioma progression through potentiating the activity of the HGF/SF autocrine pathway. *Oncogene*. 2007; 26(38):5577–5586.
34. Guven E, Afzal M, Kazmi I. Screening the significant hub genes by comparing tumor cells, normoxic and hypoxic glioblastoma stem-like cell lines using Co-expression analysis in glioblastoma. *Genes (Basel)*. 2022; 13(3):518.
35. Musumeci G, Castorina A, Magro G, et al. Enhanced expression of CD31/platelet endothelial cell adhesion molecule 1 (PECAM1) correlates with hypoxia inducible factor-1 alpha (HIF-1alpha) in human glioblastoma multiforme. *Exp Cell Res*. 2015; 339(2):407–416.
36. Liu S, Zhang C, Maimela NR, et al. Molecular and clinical characterization of CD163 expression via large-scale analysis in glioma. *Oncoimmunology*. 2019; 8(7):e16014781601478.
37. Jiang K, Wang YP, Wang XD, et al. Fms related tyrosine kinase 1 (Flt1) functions as an oncogene and regulates glioblastoma cell metastasis by regulating sonic hedgehog signaling. *Am. J. Cancer Res*. 2017; 7(5):1164–1176.
38. Pilgaard L, Mortensen JH, Henriksen M, et al. Cripto-1 expression in glioblastoma multiforme. *Brain Pathol*. 2014; 24(4):360–370.
39. Li C, Cho HJ, Yamashita D, et al. Tumor edge-to-core transition promotes malignancy in primary-to-recurrent glioblastoma progression in a PLAGL1/CD109-mediated mechanism. *Neurooncol Adv*. 2020; 2(1):vdaa163.
40. Wang H, Liu Z, Li A, et al. COL4A1 as a novel oncogene associated with the clinical characteristics of malignancy predicts poor prognosis in glioma. *Exp. Ther. Med*. 2021; 22(5):1224.
41. Pencheva N, de Gooijer MC, Vis DJ, et al. Identification of a druggable pathway controlling glioblastoma invasiveness. *Cell Rep*. 2017; 20(1):48–60.
42. Hughes JD, Fattahi N, Van Gompel J, et al. Higher-resolution magnetic resonance elastography in meningiomas to determine intratumoral consistency. *Neurosurgery*. 2015; 77(4):653–8; discussion 658. discussion 658659.

43. Hughes JD, Fattahi N, Van Gompel J, Arani A, Ehman R, Huston J, 3rd. Magnetic resonance elastography detects tumoral consistency in pituitary macroadenomas. *Pituitary*. 2016; 19(3):286–292.
44. Reiss-Zimmermann M, Streitberger KJ, Sack I, et al. High resolution imaging of viscoelastic properties of intracranial tumours by multi-frequency magnetic resonance elastography. *Clin Neuroradiol*. 2015; 25(4):371–378.
45. Fuster-Garcia E, Thokle Hovden I, Flogstad Svensson S, et al. Quantification of tissue compression identifies high-grade glioma patients with reduced survival. *Cancers (Basel)*. 2022; 14(7):1725.
46. Nia HT, Liu H, Seano G, et al. Solid stress and elastic energy as measures of tumour mechanopathology. *Nat Biomed Eng*. 2016; 1:0004. doi: 10.1038/s41551-016-0004. Epub 2016 Nov 28.
47. Capilnasiu A, Hadjicharalambous M, Fovargue D, et al. Magnetic resonance elastography in nonlinear viscoelastic materials under load. *Biomech Model Mechanobiol*. 2019; 18(1):111–135.
48. Pogoda K, Chin L, Georges PC, et al. Compression stiffening of brain and its effect on mechanosensing by glioma cells. *New J Phys*. 2014; 16:075002.